Andrzej Michalak,
Maciej Kuchar,
Zbigniew Mikołajczyk

Simulation Tests of the Feeding System Dynamics on a Warp Knitting Machine with Four Needle Bars

DOI: 10.5604/12303666.1152744

Department of Knitting Technology
Lodz University of Technology
ul. Żeromskiego 116, 90-924 Łódź, Poland
E-mail: andrzej.michalak@p.lodz.pl

Abstract
The article describes simulation tests of the basic element forming a spacer knitted structure in a newly-designed warp knitting machine with 4 guide needle bars. It refers to a concept of forming 3D knitted fabrics already developed. In the first part of the article, the introduction, a geometric-kinematic model of the feeding and knitting zones is described. In the next part, the main one, a dynamic model of the key area isolated, that is the arrangement: beam–whip roll–guide needle bar of the filling, is presented. The method of performing simulation tests of the model is described. Its susceptibility to input values in the range of values accepted was studied. The times of phases of the kinematic cycle, stiffness, damping, initial load of the model elements and their mass were changed, variations in the initial values were registered: forces in warp threads, as well as the driving force and power. The significance of the research results for further stages of constructing 3D warp knitting machines, mainly for the selection of driving actuators of the machine, is highlighted.

Key words: *3D warp knitting machine, geometric-kinematic model, dynamic model, filling needle bars, simulation tests.*

Introduction

The analysis presented below is a development and continuation of the patented concept [1] of manufacturing a 3D spatial knitted fabric. Due to the fact that the solution is highly innovative [2, 3], there is a lack of literature on the subject, apart from a reference to distance knitted fabrics [5]. Currently simulation studies are being performed, the results of which will be used to construct an experimental stand, and next a prototype of a warp knitting machine [4]. Current research tests focus on determining mechanical parameters of the drive (force and power) and also technological strength parameters - forces occurring in warp threads of the inner layer of a knitted fabric. In the first variant, the simplest possible geometrical form of the product was selected, i.e. a knitted fabric of rectangular cross-section square (see ***Figure 1***).

The knitted fabric is constructed from two pairs of side walls arranged opposite each other and a filling connecting them. A computer model of the machine forming the structure adopted was constructed. The model takes into account two basic technological zones of the machine, i.e. knitting and feeding zones. Looking further ahead, this model will be expanded to a collecting zone, which at the current stage of the analysis has been deliberately omitted. In comparison to a knitting machine forming a flat knitted fabric, the fundamental difference in the structure is the presence of additional needle bars of the filling, leading threads of the inner layer of a 3D knitted fabric. The guides of these needle bars move between the side walls of the knitted fabric. A warp thread led connects the opposite side walls and fills the space between them. Forming an internal spatial structure in two orthogonal directions of the threadconfiguration is a fundamental novelty with respect to distance knitted fabrics [5]. Also compared to the classic warp knitting machine, the far greater (due to filling a knitted fabric volume) consumption of warp thread per one cycle imposes the necessity of a thorough analysis of its load.

Preliminary assumptions accepted regarding the geometric dimensions and kinematics enable to state that the movement of guide needle bars of the filling and its synchronisation with the movement of other elements will probably have the greatest impact on the efficiency of the warp knitting machine and its performance [3, 4]. For this reason it is expedient to conduct simulation dynamic tests of these knitting elements first, before performing the next tests planned.

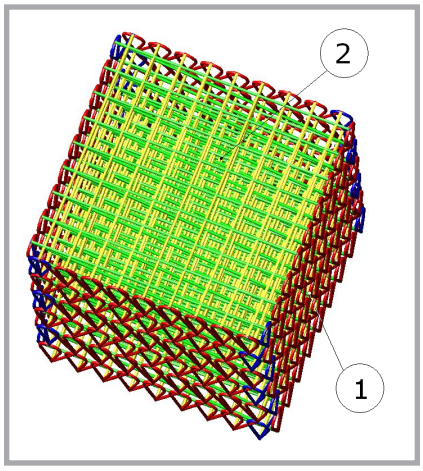

Figure 1. *3D knitted fabric of open structure [1]: 1 – side walls 2 - filling, not closed from the top and bottom.*

Geometric-kinematic model of feeding and knitting zones of a 3D warp knitting machine

In ***Figure 2.b*** (see page 128), directions *"I"* and *"II"* refer to the planes - sections adopted, in which, from a technological point of view, the process of knitting the walls and links of the filling looks identical, however it is shifted in time by half a cycle. The formation of two opposing sides of a 3D knitted fabric and their links – the filling, separately in plane *"I"* or *"II"* is performed similarly to the method of creating a three-layer distance knitted fabric [5]. The combination of using this method simultaneously in two perpendicular planes enables to form a spatial structure, which in this case consists of four identical walls connected with each other with the links' loops of the filling. In each plane *"I"* and *"II"* the knitting elements are two needle bars (3), two sinker bars (4), two guide needle bars of the walls (2) and one guide needle bar of the filling (1). Sliders of the needle bars (1) move along the guide rails (5) over a distance of 120 mm (maximum over 160 mm - cross section dimensions of a knit-

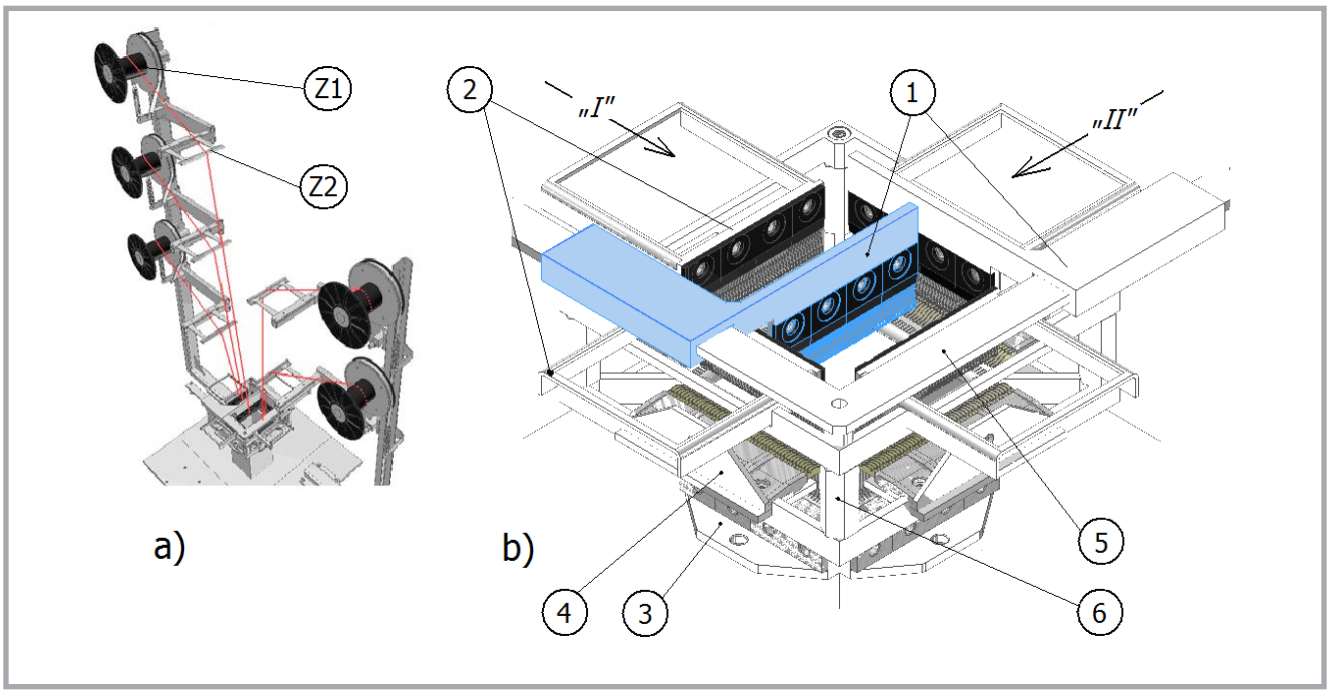

Figure 2. *Geometric-kinematic model of a 3D warp knitting machine: a) – feeding zone (only elements present in 'I' plane are shown, Z1 – beam, Z2 – whip roll), b) – knitting zone (without drive, 1 - guide needle bars of the filling, 2 – guide needle bars of the walls, 3 – needle bar, 4 – sinker bar, 5 – guide rail of guide needle bars of the filling, 6 – body).*

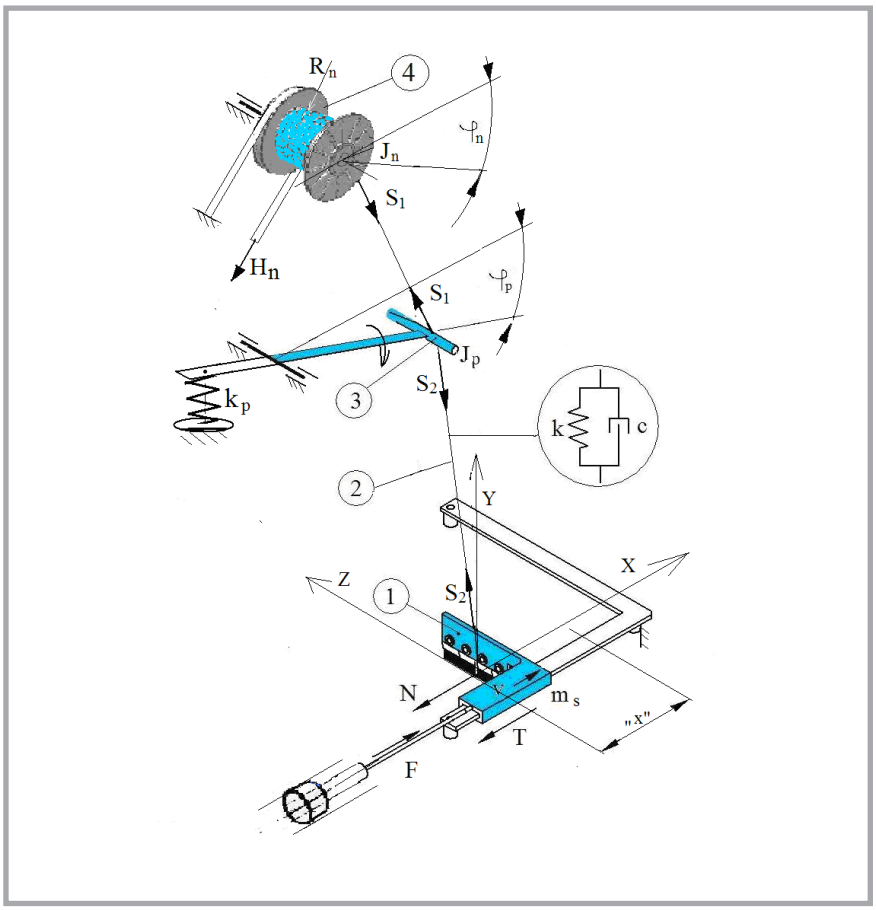

Figure 3. *Dynamic model of the feeding system of a guide needle bar of the filling; „x"- shift of the slider, v – momentary speed of the slider, m_s – mass of the slider with a guide needle bar, k – rigidity of warp, c - damping coefficient of warp, k_p – rigidity of the whip roll, φ_p – angle of rotation of the whip roll, J_p – moment of inertia of the whip roll, φ_n – angle of rotation of the beam, J_n - moment of inertia of the beam, R_n – radius of the beam, H_n – braking force, N, S_1, S_2 – forces in the warp, T – frictional force slider-guide, F – driving force of the slider.*

ted fabric). The dynamics of the movement of the guide needle bars (1), with a shift several times greater than a typical shift of other knitting elements (2, 3, 4), generates the main constraints in construction and speed. The times of shifts adopted in the analysis correspond to an average capability of 300 cycles/min, and will be optimised in the following stages.

Dynamic model of the feeding system of guide needle bars of the filling

In ***Figure 3***, a dynamic model of the feeding system of a guide needle bar of the filling is presented. The model consists of four basic elements: a slider with a guide needle bar (1), moving along the guide rail ((5) on ***Figure 2.b***), warp threads (2) between the warp beam and the edge of the knitted fabric (Z axis line), rotary-tilting whip roll (3), and warp beam (4). In its structure the model is similar to those known from literature [6, 11]. The main difference is the presence of a slider with a guide needle bar, which performs horizontal to-and-fro movement of shift "*x*".

Parameters of rigidity and damping were introduced in the model, including the rheological properties of warp threads and mass in motion. A warp thread in the model is treated as weightless. A parallel

connection of the damping section and rigidity was proposed as a rheological model of a stretched warp thread (Kelvin - Voigt model) [8].

The driving force F, of required maximum values and nature of instantaneous changes, performs the kinematics of the slider (1) movement assumed at a speed v and forward and backward shift "x", with needle bars leading the warp threads (2). A summary of tensions of all 48 threads (which, in the Figure, are presented as a single line for a clear view) drawn-in through the guide needle bar is given as follows:

N – in section between the edge of the knitted fabric (line of the beginning of the cycle, overlaying the Z axis in the Figure) and guide needle bar,

$S1$ – in section between the beam and whip roll,

$S2$ – in section between the whip roll and guide needle bar.Resistance to the movement of the slider with a guide needle bar and the driving force F is a variable in the time resultant force, which is a sum of:

- the frictional force T in the guide rail (resulting from the summary pressure from external forces loading the slider),
- warp tension N - parallel to the direction of movement X,
- S_{2X} force - projected in the direction of X of the variable (also in the angle of operation) tension S_2
- dynamic forces of the masses in motion (mass of the slider with a guide needle bar and a movable part of the driving actuator).

All the forces included in the model act within the plane X-Y (corresponding to the technological plane designated as *"I"* in the description in the chapter 'Geometric-kinematic model of feeding and knitting zones of a 3D warp knitting machine'.

At the time of the forward and then backward shift of the slider with a guide needle bar, warp threads are arranged between the walls of the knitted fabric, forming its filling. Associated with these temporary changes in the length of the individual sections of warp thread are compensations in the form of a deflection of the whip-roll. After crossing the boundary value of thread tension (set by the brake of the beam), the warp thread unwinds in an amount corresponding to a longer period of time to the length of thread knitted-in the knitted fabric. In this model the rotation of the beam of angle φ_n corresponds to this quantity in a short period of time. The rheology of the threads are defined by their rigidity k and damping coefficient c [10, 12]. The damping of the beam was omitted as practically non-existent, and the beam arm was assumed to be rigid, with a rotational fastening of torsional rigidity k_p.

The predetermined distance and speed in the phases of the slider's movement forward, backwards, and stopping are presented in ***Figure 4***.

For the elements of the model of the beam, whip roll and slider, the equations of movement can be written as (1, 2, 3):

$$J_n\ddot{\varphi}_n + M_{nh} = M_n, \quad (1)$$

$$J_p\ddot{\varphi}_p + M_{ps} = M_p, \quad (2)$$

$$m_s\ddot{x} + N + S_{2x} + T = F, \quad (3)$$

Forces in the threads are described by dependencies (4):

$$S_2 = S_1 e^{\mu_0\alpha_1}, \; N = S_2 e^{\mu_0\alpha_2} \quad (4)$$

where,

M_{nh} - braking torque of the beam (mainly of force H_n but also of force S_1 and weight of the beam),

M_n - moment of warp thread tension causing a rotation of the beam (of force S_1),

M_{ps} - moment of torsional rigidity of the whip roll (of the angle of inclination φ_p),

M_p - moment of warp thread tension causing a movement of the whip roll (of forces S_1 and S_2),

S_{2x} - S_2 force projection in direction of slider movement x.

The relationship between the values occurring in ***Equations 1 - 3*** result from the dynamic model shown in ***Figure 3***, by adopting specific values of rheological parameters of the thread. Threads in the model are the elements linking the beam, whip roll and slider.

It was assumed that the cycle of movement of the guide needle bar includes a forward shift, transient stop and return to the starting position (***Figure 4***). The times of forward and backward shifts are approximately equal to each other, τ = 0.1, 0.05 & 0.03 s in three time trials, while the time of the transient stop is, for technological reasons (forming a loop, side laps of needle bars), always the same and equal to 0.1s. The cycle time is equal to 0.3, 0.2, & 0.16 s, respectively.

The following values of model parameters were adopted [6, 10, 11, 14]:

- rigidity of the whip roll k_p = 0.03 - 0.2 Nm/deg,
- warp rigidity k = 8 – 300 kN/m (upper values correspond to the technical yarns),
- damping coefficient of warp thread c_0 = 0.2 – 20 kNs/m,
- friction coefficient between the slider and guide rail μ = 0.04 - 0.30,
- friction coefficient of a warp thread on the whip roll and of a warp thread in the needle bar eyelet μ_0 = 0.08 - 0.30,
- friction coefficient of the beam reel μ_n = 0.15,
- mass of the slider with a needle bar guide and movable part of the actuator m_s = 0.6 - 1.8 kg,
- mass of whip roll m_p = 0.018 - 0.176 kg,
- mass of beam m_n: 0.1 – 0.5 kg,
- shift of slider 60, 120 (basic), 180 mm,
- initial tension of warp thread S_0: 10 N (20 cN per 1 thread) – 80 N (160 cN),
- angle of wrapping whip roll with warp thread α_1 = 30°,
- angle of wrapping needle bar eyelet with warp thread α_2 =180°,
- radius of beam Rn = 0.08 m - 0.03 m.

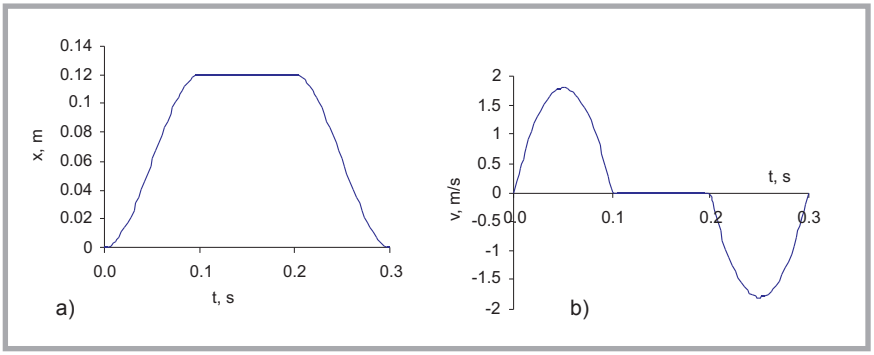

Figure 4. *Predetermined distance (a) and speed (b) of the slider with a guide needle bar.*

Results of simulation tests

Instantaneous values of moments and forces according to dependencies (1 - 4) were obtained using the dynamic simulation module of Autodesk Inventor software. Exemplary results are presented in the following Figures.

Figure 5 shows the characteristics of forces acting on the slider according to ***Equation 3***. For a time of shift $\tau = 0.1$ s (***Figure 5.a***), the forces that significantly and comparably act against the movement of the slider are the following: a load with warp thread from the edge of the knitted fabric *N* and frictional force of the slider on the guide rail *T*. To a lesser degree the load is composed of a component in the *X* direction of warp thread tension from the whip roll side S_{2X}. From the angle of the technological inclination of the thread (S_2 deviation in regard to *Y* - ***Figure 3***), it results that this force is directed opposite to the *X*-axis in both phases of the movement, both forwards and backwards, which means that in the phase of the return movement of the slider, when the sense of *F* is reversed, it becomes a driving component.

With the shortest (analyzed) time of a shift $\tau = 0.03$ s (***Figure 5.b***), the share of the resisting forces associated with the influence of the warp thread on the slider (technological resistance) in relation to the driving force clearly decreased, which indicates the dominance of dynamic forces.

Figure 6 presents instantaneous values of the moments of the beam *Mn* and whip roll M_p in the same variants of the longest and shortest time of the shift analysed. The characteristics of moments are shown in relation to an increase in the beam twist angle φ_n. Momentary drops in warp thread tension at turning points of the shift, visible for small values of τ (***Figure 6.b***), are caused by the inertia of the beam in the moments of its movement (starting and stopping), in response to crossing the boundary values of thread tension adjusted with a brake. These changes are suppressed in the warp thread and practically do not transfer to the slider (***Figure 5.b***). It means that in the model constructed, the beam acts towards the drive as an immobile point of thread fastening, which is also consistent with the assumptions of some of the similar models known from the literature [6]

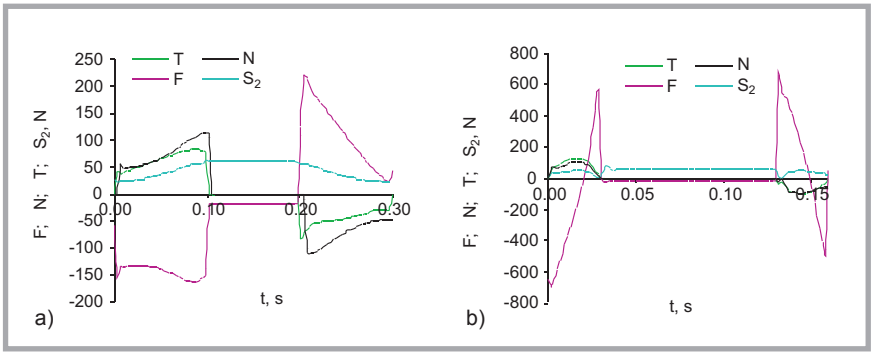

Figure 5. *Characteristics of forces loading the slider of a guide needle bar: driving force F and resistant forces N, T, S_2: a) time of shift $\tau = 0.1$ s (cycle time 0.3 s), $k_p = 0.03$ Nm/deg, $k = 8$ N/mm, $x = 120$ mm, b) time of shift $\tau = 0.03$ s (cycle time 0.16 s), $k_p = 0.2$ Nm/deg, $k = 200$ kN/m, $x = 120$ mm.*

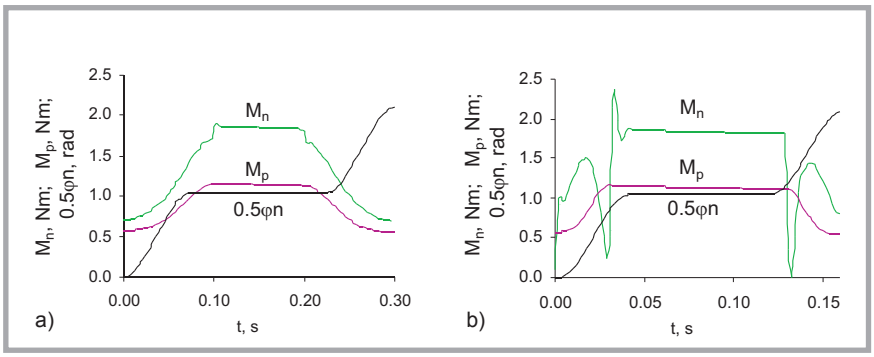

Figure 6. *Characteristics of moments of warp tensions for the beam M_n and whip roll M_p: a) time of shift $\tau = 0.1$ s, b) time of shift $\tau = 0.03$ s.*

describing the dynamics of the feeding system at short intervals of time.

A slight response of the whip roll (***Figure 6.b***), however, results from the geometry of the warp thread (smaller angle of wrapping) near the turning point of the slider.

Due to the proper selection of the driving actuator, the value of force *F* in relation to the speed of movement of the slider is important [7, 9, 13, 16]. ***Figure 7*** shows characteristics of the driving force *F* in a single cycle of slider movement in terms of phase, at different times of shift τ. Differences between the shapes of the loop corresponding to the slider shifts forward and backward can be seen, wherein they are greater for a longer time and decrease with a decrease in time. This indicates the decreasing effect of technological resistance in relation to the dynamic forces. The maximum values of the driving force *F* are similar for the forward and backward movement in each case of time τ. As a result of the impact of the inertial force, the peak value of the driving force increases from 220 N in the first variant to 700 N in the third with a decrease in the time of the shift. The characteristics also show that for the case of a short time $\tau = 0.05$ s and even more so for the shortest time $\tau = 0.03$ s, the force *F* changes its sense before reaching the end value of the shift range. This applies to both forward and backward movements.

The instantaneous demand of the slider system on the driving power P was calculated as a product of instantaneous values of the driving force and the speed of the slider:

$$P = F \cdot v \tag{5}$$

Characteristics of instantaneous values of power *P* as a function of time are shown in ***Figure 8***. With a double decrease in the time of a shift, the peak value of the driving power increases three times. For a longer time $\tau = 0.1$ s in the braking phase, the power decreases, while for a short time, and especially for the shortest time analysed, the braking involves a change in the sense of the driving force to the opposite one before reaching the turning point.

Similar simulations to those in ***Figures 6*** and ***7*** were repeated several times, each time changing another dynamic param-

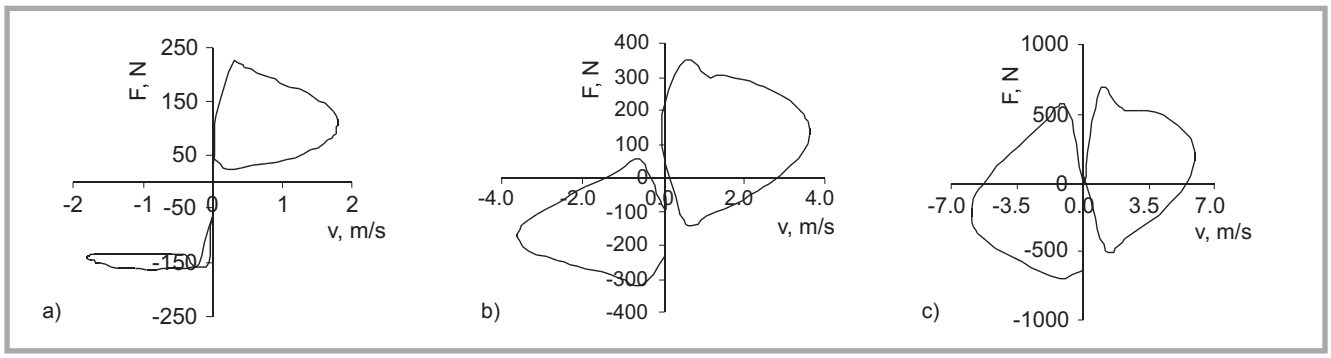

Figure 7. *Instantaneous values of the driving force F as a function of the slider speed, times of shifts: a) τ = 0.1 s, b) τ = 0.05 s, c) τ = 0.03 s; k_p= 0.2 Nm/deg, k = 200 kN/m.*

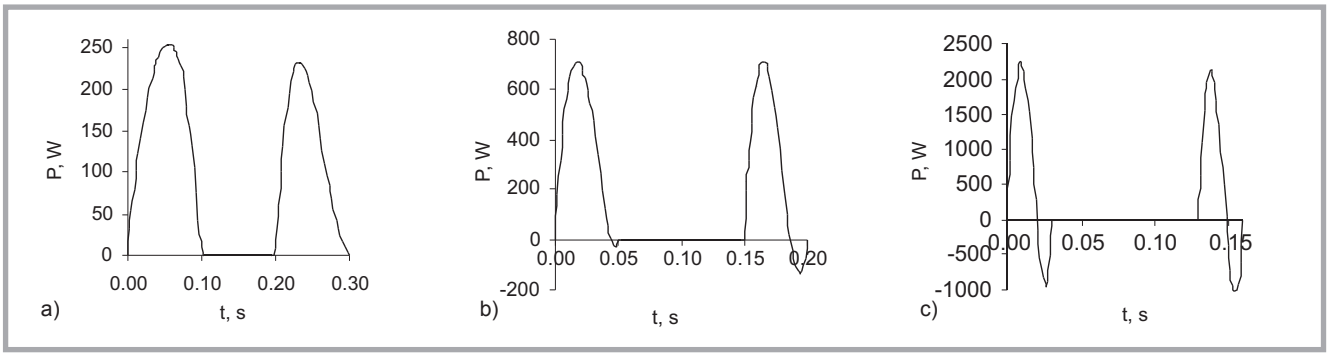

Figure 8. *Characteristics of instantenuous values of the power of the dynamic system of the slider; times of shifts: a) τ =0.1 s, b) τ = 0.05 s, c) τ = 0.03 s, k_p= 0.2 Nm/deg, k =200 kN/m.*

eter. Summary results of the analysis carried out under varying dynamic conditions are presented in the graphs grouped in ***Figures 9*** and ***10***, which describe only those parameters whose influence was considered significant. Thus, for example, with respect to the beam, only the effect of changes in its radius is given.

Figure 9 shows a graphs of the warp thread load under variable dynamic conditions. ***Figures 9.a, 9.b*** & ***9.c*** show the influence of the mass and rigidity of the whip roll and of a shift on the value of the maximum load of the warp thread S_{2m}. This load increases linearly with a decrease in the mass of the whip roll and an increase in its rigidity, and nonlinearly

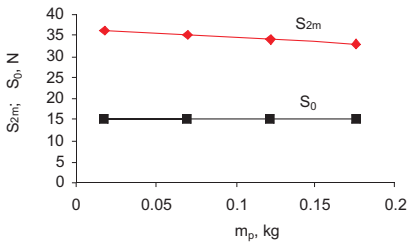

a) ***m_p*** *(τ = 0.05 s, k = 200 kN/m, k_p = 0.05 Nm/deg, X = 0.12 m, μ = 0.14 - 0.08, μ_0 = 0.2 - 0.17, c_0 = 200 Ns/m)*

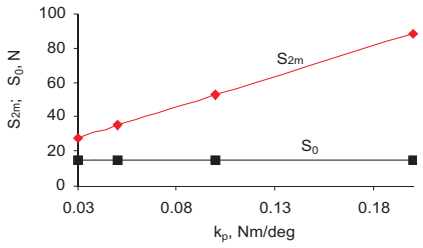

b) ***k_p*** *(τ = 0.05 s, k = 200 kN/m, μ = 0.14 - 0.08, μ_0 = 0.2 - 0.17, X = 0.12 m, c_0 = 200 Ns/m)*

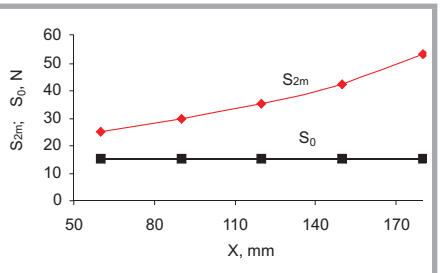

c) ***x*** *(τ = 0.05 s, k = 200 kN/m, k_p = 0.05Nm/deg, μ = 0.14 - 0.08, μ_0 = 0.2 - 0.17, X = 120, c_0 = 200 Ns/m)*

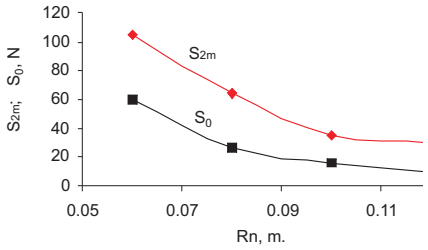

d) ***Rn*** *(τ = 0.05 s, k = 200 kN/m, kp = 0.05 Nm/deg, X = 0.12 m, μ = 0.14 - 0.08, μ_0 = 0.2 - 0.17)*

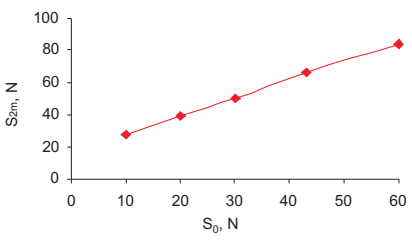

e) ***S_0*** *(τ = 0.05 s, k = 200 kN/m, k_p = 0.05 Nm/deg, X = 0.12 m, μ = 0.14 - 0.08, μ_0 = 0.2 - 0.17, c_0 = 200 Ns/m)*

Figure 9. *Maximum warp tension S_{2m} and initial tension S_0 as a function of the slider as a function of different dynamic parameters.*

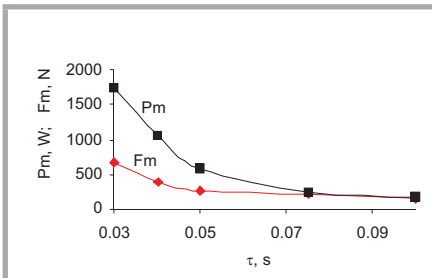

a) ***τ*** *(k_p = 0.05 Nm/deg, k = 200 kN/m, μ = 0.14 - 0.08, μ_0 = 0.2 - 0.17, X = 0.12 m, c_0 = 200 Ns/m, S_0 = 10 N)*

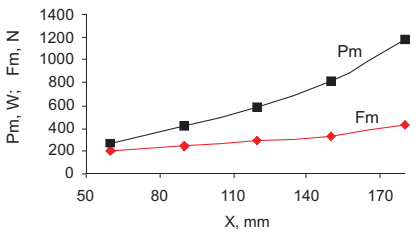

b) ***x*** *(τ = 0.05 s, k = 200 kN/m, k_p = 0.05 Nm/deg, μ = 0.14 - 0.08, μ_0 = 0.2 - 0.17, X = 0.12 m, c_0 = 200 Ns/m, S_0 = 10 N)*

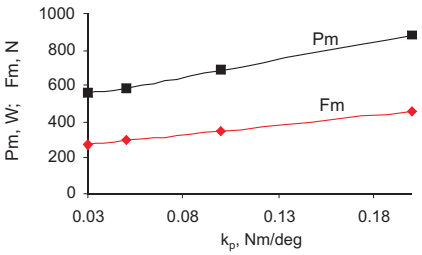

c) ***k_p*** *(τ = 0.05 s, k = 200 kN/m, μ = 0.14 - 0.08, μ_0 = 0.2 - 0.17, X = 0.12 m, c_0 = 200 Ns/m, S_0 = 15 N)*

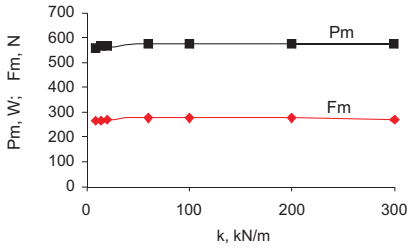

d) ***k*** *(τ = 0.05 s, k_p = 0.05 Nm/deg, μ = 0.14 - 0.08, μ_0 = 0.2 - 0.17, X = 0.12 m, c_0 = 200 Ns/m, S_0 = 15 N),*

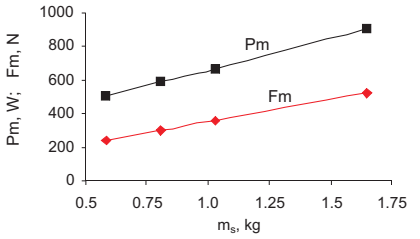

e) ***μ*** *(τ = 0.05 s, k = 200 kN/m, k_p = 0.05 Nm/deg, X = 0.12 m, μ_0 = 0.2 - 0.17, c_0 = 200 Ns/m, S_o = 15N)*

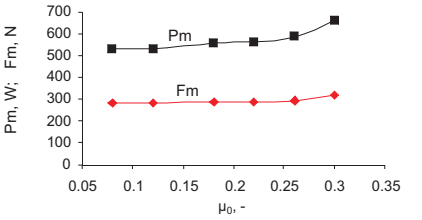

f) ***μ_o*** *(τ = 0.05 s, k = 200 kN/m, k_p = 0.05 Nm/deg, X = 0.12 m, μ = 0.14 - 0.08, c_0 = 200 Ns/m, S_0 = 15 N)*

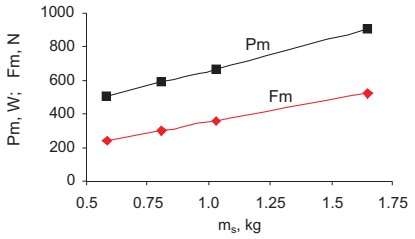

g) ***m_s*** *(τ = 0.05 s, k = 200 kN/m, k_p = 0.05 Nm/deg, X = 0.12 m, μ = 0.14 - 0.08, μ_0 = 0.2 - 0.17, c_0 = 200 Ns/m, S_0 = 15 N)*

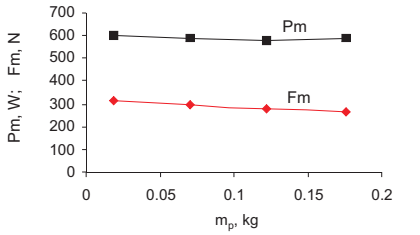

h) ***m_p*** *(τ = 0.05 s, k = 200 kN/m, k_p = 0.05 Nm/deg, X = 0.12 m, μ = 0.14 - 0.08, μ_0 = 0.2 - 0.17, c_0 = 200 Ns/m, S_0 = 15 N)*

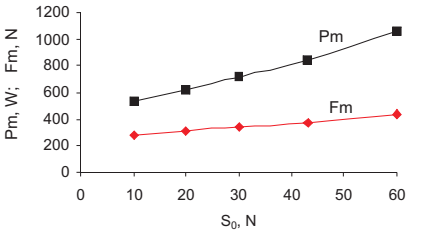

i) ***S_0*** *(τ = 0.05 s, k = 200 kN/m, k_p = 0.05 Nm/deg, X = 0.12 m, μ = 0.14 - 0.08, μ_0 = 0.2 - 0.17, c_0 = 200 Ns/m)*

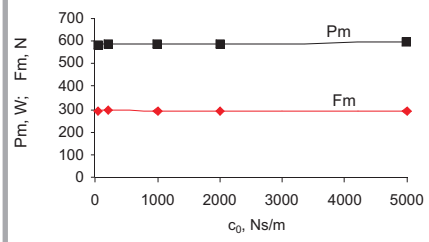

j) ***c_o*** *(τ = 0.05 s, k = 200 kN/m, k_p = 0.05 Nm/deg, X = 0.12 m, μ = 0.14 - 0.08, μ_0 = 0.2 - 0.17, S_0 = 15 N)*

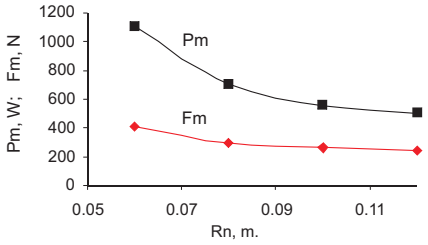

k) ***R_n*** *(τ = 0.05 s, k = 200 kN/m, k_p = 0.05 Nm/deg, X = 0.12 m, μ = 0.14 - 0.08, μ_0 = 0.2 - 0.17, S_0 = 15 N)*

Figure 10. *Peak values of force F (Fm) and driving power P (Pm) of the slider as a function of different dynamic parameters.*

with an increase in the shift of the slider. The load of warp thread decreases (***Figure 9.d***) with an increase in the radius and mass of the beam associated, at a constant braking torque. It is advantageous from the point of view of the warp load to reduce the initial tension as shown in ***Figure 9.e***. A noticeable influence of other parameters analysed *(τ, μ, μo, k)* on the force S_2 is not observed. The influence of various dynamic parameters sequentially introduced (in chapter *Dynamic model of the feeding system of guide needle bars of the filling*) on the maximum instantaneous values of the power *P* of the drive and driving force *F* was analysed. The test results are shown in ***Figure 10***.

Figure 10.a presents the influence of the time of the shift. When decreasing the time of the shift below τ = 0.1 s, an adverse effect of the inertial force is revealed. Both the values of the force and power of the slider drive increase, and for the shift time τ = 0.03 s these values increased several times (e.g. values of the power increased eight times). A similar effect is caused by increasing the range of the shift *x* with the same time τ, as shown in ***Figure 10.b***. For the basic shift of 120 mm, the peak value of power is 600 W. The following figures show the influence of the rigidity of the whip roll (***Figure 10.c***) and warp thread (***Figure 10.d***). A reduction in the rigidity of the whip roll is advantageous for the dynamic load of the warp thread, which translates into the load of the slider during the movement, thus reducing the

Table 1. Average values.

$\mu_{max} - \mu_{min}$	0.04	0.14 - 0.08	0.2 - 0.12	0.24 - 0.16	0.3 - 0.2
μ_{av}	**0.04**	**0.11**	**0.16**	**0.20**	**0.25**

value of the force and driving power. In contrast, an increase in the rigidity of the warp thread within the range from 50 N/mm up to 300 N/mm (technical yarns) does not give a noticeable increase in the driving force and power. Results of the analysis of frictional properties of yarns and machine components are presented. The influence of average values of the friction coefficient for configuration yarn-metal and metal-metal are shown in the graphs (***Figure 10.e*** and ***10.f***). Values of the friction coefficient of warp thread in the guide needle bar eyelets result from the literature data available [12, 15] and were adopted as values irrespective of the velocity. Values of friction coefficients of the slider-guide were adopted within the ranges. A change from static to kinematic friction is associated with a decrease in its value along with increasing speed [17]. The ranges corresponding to average values were adopted for the analysis, as given in ***Table 1***.

The influence of mass changes was analysed for both the slider and whip roll, which in practice involves the use of different materials for these elements and slightly different shapes. The impact of the slider mass proved to be significant (***Figure 10.g***), while that of the whip roll mass (***Figure 10.h***) is small. The next graph (***Figure 10.i***) shows that, as expected, an increase in the initial tension of warp thread S_o leads to an increase in the force F and power P of the drive, while a six-fold increase in S_o corresponds to a two-fold increase in the driving power of the characteristics similar to linear. ***Figure 10.j*** shows that (as in the case of the warp thread rigidity) the damping coefficient of warp thread, characterising a particular yarn, is relevant only within the range of small values of up to approx. 300 Ns/m. Its further growth, even tenfold, does not affect the value of the force and power of the drive. The final input quantity, the impact of which was tested, is the radius of the beam. Assuming a constant braking torque (set), along with a decrease in the radius of the beam, the warp thread tension increases as well as the technological resistance of the slider, the consequence of which is an increase in the parameters of the drive, as presented in ***Figure 10.k***.

Determination of the characteristics of the power and forces for certain times of shifts of the slider with a needle bar guide enables to select pneumatic or electric actuators with optimal fit. The peak values of power and speed of the slider are the output parameters for selection of the driving actuator [9, 13]. For example, for time τ equal to 0.1, 0.05 & 0.03 s the power is 250, 700 and 2200 W, respectively. These values are at a similar level for both warp threads made from classic yarns of smaller rigidity and - which is worth emphasising – made from technical yarns, of a rigidity several times larger.

Conclusions

1. The main resistant forces of a slider with a guide needle bar are technological resistances for shift times within the range: 0.1 - 0.05 s.
2. The resistant forces of the slider are small compared to its dynamic forces for the time of the shift within the range 0.03 - 0.05 s.
3. At the same time, for a range of shorter times of the shift, with a gradual decrease in time, the instantaneous driving power increases exponentially up to approx. 2 kW.
4. The immediate effect of reducing the time of the shift is also a gradual increase in the similarity of phase characteristics of the slider's movement forward and backward.
5. The beneficial effect on the load of warp thread and technological resistance of the slider is shown by a reduction in the rigidity of the whip roll and initial tension of the warp thread.
6. An increase in the rigidity of the warp thread above 50 kN/m (for technical yarns) does not increase the load and driving force.
7. The system can be modelled, for short times of shifts, omitting the impact of inertia of the beam and replacing it with an immobile point of warp thread fastening.
8. A five-fold reduction in the coefficient of friction between the slider and guide rail reduces the force and driving power by approx. 30%.
9. An increase in the beam radius, assuming a constant braking moment, has a beneficial effect on the parameters of the drive and load of the warp thread.

References

1. Mikołajczyk Z, Pieklak K, Golczyk A, Wiater Z. *Knit spatial product (in Polish).* P-386074. Polish Patent Office 25.09.2014.
2. Pieklak K, Mikołajczyk Z. Original concept of a new multicomb warp-knitting machine for manufacturing spatial knitted fabrics. *Fibres & Textiles in Eastern Europe* 2009; 17, 3(74): 76 – 80.
3. Michalak A, Mikołajczyk Z. The concept of building a warp knitting machine for 3D knitting desing and construction assumptions (in Polish). In: *XVI Scientific Conference of the Faculty of Material Technologies and Textile Design* 2013, TUL.
4. Michalak A, Kuchar M, Mikołajczyk Z. Constructive assumptions of a new four-comb warp – knitting machine. In: *47th IFKT Congress,* 2014, Izmir, Turkey.
5. Gręboswki J. Three-layer knitted fabrics (in Polish). *Przegląd Włókienniczy* 2000; 9: 37-38.
6. Kopias K. *Technologia dzianin kolumienkowych.* Ed. WNT, Warszawa, 1986, pp. 178.
7. Kossowski Z, Kuchar M, Siczek K. Analysis of the power of a oscillating motion magneto-electric inductor system working under the conditions of discontinued work (in Polish). *Przegląd Elektrotechniczny* 2007; 7-8: 20-25.
8. Kuchar M. *Vibratory Thickening of Weft Threads in a Weaving Loom – Simulation Tests. Fibres & Textiles in Eastern Europe* 2013; 21, 5(101): 59-64.
9. Heimann B, Gerth W, Popp K. Mechatronics. The components, methods, examples. Ed. PWN, 2013.
10. Mikołajczyk Z. Optimisation of the Knitting Process on Warp-Knitting Machines in the Aspect of the Properties of Modified Threads and the Vibration Frequency of the Feeding System. *Fibres & Textiles in Eastern Europe* 2011; 19, 6(89): 75-79.
11. Mikołajczyk Z. Optimisation of the Knitting Process on Warp-Knitting Machines in the Aspect of the Feeding Zone Geometry. *Fibres & Textiles in Eastern Europe* 2011; 19, 4(87): 81-88.
12. Mikołajczyk Z. Modelling of the Knitting Process with Respect to the Optimisation of the Construction Parameters of Warp-Knitting Machines. *Fibres & Textiles in Eastern Europe* 2009; 17, 2(73): 76-81.
13. Kossowski Z, Kopias K. Magnetoelectric Driving Device for Displacements of a Guide Needle Bar in a Weaving Loom. *Fibres & Textiles in Eastern Europe* 2006; 14, 2(56): 76-78.
14. Zhang H-W, Guo X-F, Li Y-L. Mechanical Properties of Ring-spun Yarn and its Strength Prediction Model. *Fibres & Textiles in Eastern Europe* 2011; 19, 3(86): 17-20.
15. Koncer P, Gürarda A, Kaplangiray B, Kanik M. The effects of sewing thread properties on the needle thread tension in an industrial sewing machine. *Tekstil ve Konfeksiyon* 2014; 24(1): 118-123.
16. Pacurari R, Csizar A, Brisan C. Basic aspects concerning modular design of reconfigurable parallel manipulators for assembly tasks at nanoscale (in Polish). *Mechanika* 2009; 2(76): 69-76.
17. Bhushan B. *Modern Tribology Handbook.* Ed. Crc Press, 2001, pp. 1690.

Received 09.07.2014 Reviewed 04.03.2015